Preparation of activated carbon from orange peel and its application for phenol removal

Loriane Aparecida de Sousa Ribeiro[1], Liana Alvares Rodrigues[2*],
Gilmar Patrocínio Thim[3]

[1,3]Instituto Tecnológico de Aeronáutica-ITA/CTA, Praça Mal. Eduardo Gomes 50, CEP 12228-900, São José dos Campos, São Paulo, Brazil.
[2]Departamento de Engenharia Química, Escola de Engenharia de Lorena-EEL/USP, Estrada Municipal do Campinho S/N, CEP 12602-810, Lorena, São Paulo, Brazil

Abstract— *Activated carbon obtained from orange peel (ACO) was used as a phenol adsorbent. ACO was characterized by X-ray diffraction, Raman spectroscopy, scanning electronic microscopy (SEM) and energy dispersive spectroscopy (EDS). The functional groups present on the sample, were determined by Boehm titration, and it was also determined the point of zero charge (pHpzc). ACO is mainly constituted by micropores, and its structure is turbostratic and lamellar with inorganic impurities. The Boehm titration indicated the basic behavior of the sample. The phenol optimum dosage was 0.1 g/50 cm³ which was determined by the adsorption study. The maximum adsorption level was in the pH range of 4-8 and its kinetics was described by a pseudo second order model. The equilibrium data have fit very well the Langmuir and Sips isotherms models.*

Keywords— *adsorption, agricultural waste, biomass, orange peel, phenol.*

I. INTRODUCTION

Brazil is the largest producer of oranges in the world, and it is responsible for about 30% of the world production[1]. Basically, almost all Brazilian´s orange production is used to produce orange juice[2].The European Union is the major consumer of orange juice, being 96% of it imported from Brazil[3]. The fruit is compounded of 50 % (w/w) of juice and the other 50 % of peel, pulp, seeds and membranes[2,4], being its peel, the primary byproduct during the orange juice processing[2]. Part of this waste material is used to produce pet food, fiber (pectin), fuel, essential oils, fertilizers, anti-oxidizing compounds and adsorbents [2,5,6]. However, the major part of the fruit after juice production becomes litter and is discarded to environment by juice industries [5]. Thus, changing the orange peel, which is a low cost agricultural waste, into a useful material, such as adsorbents that can add value to this residue and contribute to the problem of biomass disposal[7].

The phenol molecules and phenol-constituted substances are essential for several industrial processes, such as: rubber, dye, pharmaceutical and pesticide production and oil refining [8,9]. Nevertheless, their presence in water supply poses risks of water quality degradation and aquatic life death, moreover, it can inhibit the microbial community normal activities and cause carcinogenicity in animals [8,10]. Therefore, the discard of this kind of effluent is controlled by environmental offices and the maximum concentration allowed to this effluent is 0.002 mg/L [11]. The industries responsible for phenol contaminated effluent have to remove the phenol before discarding it in the environment in order to comply with the levels demanded by environmental agencies [12].

There are several methods proposed to remove phenol from industrial effluent, such as: biological treatment, adsorption on activated carbon, reverse osmosis, ionic exchange, solvent extraction, ultrasonic degradation and TiO_2 oxidation [13]. Among these methods, the adsorption process is the cheapest, simplest and fastest one for phenol removal [12]. Activated carbon is considered to be an effective method for phenol removal from contaminated effluents due to its elevated surface area, microporosity, and high adsorption capacity [14]. Nonetheless, phenol adsorption is economically unfeasible due to its elevated cost of production [7]. An alternative to reduce the activated carbon production cost is to use an abundant and low cost carbon source, such as agricultural or industrial waste to produce it [15]. Activated carbon from orange peel has been obtained with an elevated surface area and pore volume [16]. Consequently, activated carbon obtained from orange peel has emerged as a potential alternative for activated carbon production.

The main objective of this paper is to study the adsorption process of phenol in the activated carbon obtained from the orange peel. Its goal is to obtain a low cost activated carbon able to remove phenol from industrial effluent and concomitantly enhance the value of an abundant biomass and solve its disposal problem.

II.   METHODOLOGY

2.1   Synthesis of the activated carbon from orange peel (citrus sinensis)

The activated carbon was prepared following these seven steps:

1.   Rinsing it with deionized water;
2.   Drying it in an oven at 100 °C until constant mass;
3.   Milling and sieving it (4-8 mesh);
4.   Carbonizing it in a tubular furnace under argon flow, from 25 °C to 800 °C at a heating rate of 30 °C/min, which was maintained at 1073K for 1 hour;
5.   Turning off the argon flow and turning on CO_2 at 100 cm^3/min. Maintaining the samples under this condition for 3 hours;
6.   Turning off the CO_2 flow and turning on the argon at 100 cm^3/min, switching off the heating system;
7.   Milling and sieving it (325 mesh). Sample in this stage was called ACO.

2.2   Characterization

The point of zero charge (pHpzc) was determined using the methodology described in several papers [12,17,18]. ACO (0.05 g) was added to several flasks containing 25 cm^3 of KNO_3 (concentrations 10^{-1} and 10^{-2} M) solutions which the initial pH values (pHi) were adjusted in the pH range of 2–8 using 0.1 M of HCl or NaOH. Then, the equilibrium was carried out in a thermostatic linear shaker for 24 h at 298 K. The dispersions were then filtered and the final pH of the solutions (pH_f) was determined. The point of zero charge was found from a plot of ($pH_i - pH_f$) versus pH_i. The Boehm method was used to determine the amount of the oxygenated chemical groups [19], where one gram of ACO was placed in 25 cm^3 of the following aqueous solutions: sodium hydroxide, sodium carbonate, sodium ethoxide, sodium bicarbonate and hydrochloric acid. The vials were sealed, shaken for 24hs and then filtered. The filtrate was titrated with HCl or NaOH to determine the base or acid excess, respectively.

The sample morphology was observed in a Scanning Electron Microscope (SEM), Zeiss model EVO MA 10. Energy dispersive spectroscopy (EDS) measurements were carried out in an Oxford INCA Energy Microanalysis System which was incorporated to SEM. Raman spectroscopy was carried out in a Renishaw 2000 equipment using ionic laser of Ar^+ (λ=514.5 nm). Powders were analyzed in a X ray diffraction equipment, using a PANalytical X'Pert PRO MPD 3060 diffractometer, equipped with a X'celerator detector, operating at 45 kV and 25 mA with CuKα radiation. XRD patterns were collected in the 2θ range from 10 to 90º at scan speed of 0.42 º s^{-1} and step size of 0.017°.

2.3   Adsorption study

Adsorption studies were carried out in amber glass flasks of 100 cm^3, where ACO was mixed to a phenol aqueous solution (50 cm^3), being stirred in a thermostatic shaker. The supernatant solution was separated from the adsorbent by filtration. The phenol concentration in the supernatant was spectrophotometrically determined using UV−VIS absorbance spectrophotometery at 269 nm [20]. Solutions, with higher concentration than the ones detected by the spectrophotometer, were determined by dilution. Adsorption kinetics was performed using 0.1 g of ACO, in a period from 0 to 24 hours, without adjusting its pH, 25 °C and a phenol initial concentration of 1000 mg/dm^3. The pH effect was carried out using 0.1 g of ACO, during 3hs, with a pH range between 2 and 12, at a temperature of 25 °C and a phenol initial concentration of 1000 mg/dm^3. Dosage effect was accomplished using ACO mass range between 0.1 and 0.5 g, bath time of 3 hours, without adjusting its pH, at a temperature of 25 °C and a phenol initial concentration of 1000 mg/dm^3. The isotherm adsorption was obtained using 0.1 g of ACO, bath time of 3 hours, without adjusting its pH, at a temperature of 25 °C and phenol initial concentration ranging from 50 to 1000 mg/L.

III.   RESULTS AND DISCUSSION

3.1   Characterization

The pH_{PZC} is the pH in which the surface charge of a material is zero. The surface of an amphoretic material is positively charged if the medium pH is lower than pH_{PZC}. On the other hand, it is negatively charged if the medium pH is higher than pH_{PZC} [7]. The pH_{PZC} of ACO is 10.5, indicating a basic character in water.

The number of basic sites on the ACO surface was determined from the amount of hydrochloric acid that reacted with the activated carbon. The number of acid sites was determined under the following assumptions: a) there are only carboxylic, lactonic, phenolic and carbonyl groups on ACO, b) NaOH neutralizes the carboxylic, lactonic and phenolic groups; c)

Na_2CO_3 neutralizes the carboxylic and lactonic groups; d) $NaHCO_3$ neutralizes only the carboxylic groups; and e) $NaOC_2H_5$ neutralizes the carbonyl (quinoid-type), carboxylic, lactonic and phenolic groups. This procedure is called Boehm titration and is described in several papers [7,19]. Table 1 shows the amount of acid and basic groups present on the ACO surface. The amount of basic groups (3.38) is higher than the acid groups (1.19). Therefore, the sample is predominantly basic.

TABLE 1
SURFACE FUNCTIONAL GROUPS FOR ACO

Acid sites				Basic sites (mmol g^{-1})
Carboxyl (mmol g^{-1})	Lactones (mmol g^{-1})	Phenols (mmol g^{-1})	Carbonyl (quinoid-type) (mmol g^{-1})	
0.00	0.00	1.19	0.00	3.38

Fig. 1 shows the Raman spectrum of ACO sample, which shows peaks centered at 1361 and 1583 cm^{-1}. These peaks are attributed to the D band (1200-1400 cm^{-1}) and G band (1500-1600 cm^{-1}), respectively [22].
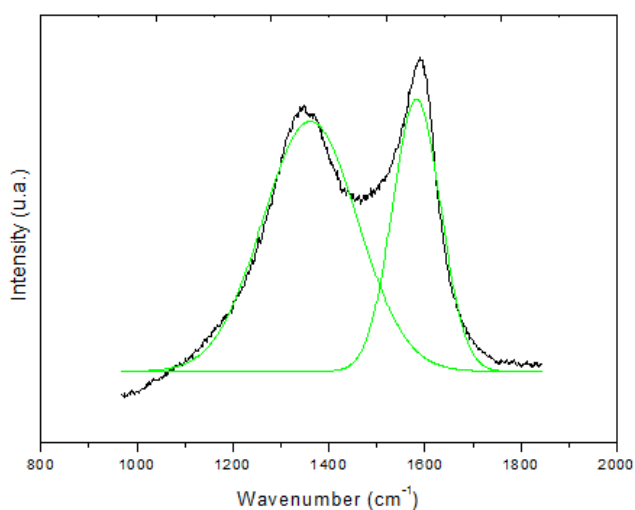
FIGURE 1. RAMAN PROFILE OF THE ACO SAMPLE
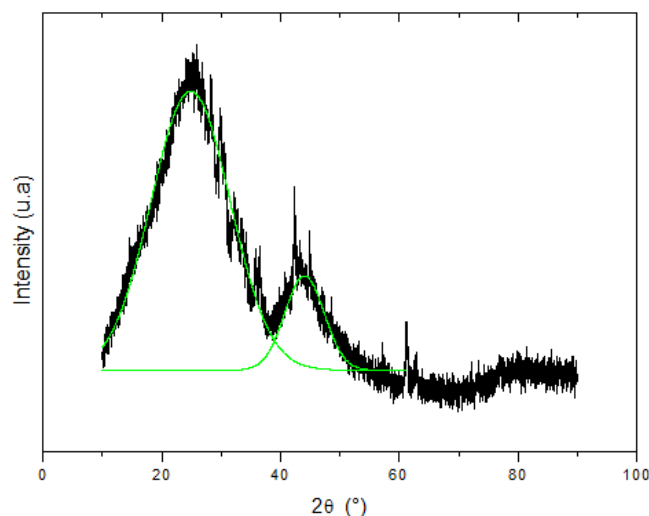
FIGURE 2. X RAY DIFFRACTOGRAM OF THE ACO SAMPLE

A Gaussian deconvolution method was used to obtain the half width of band G (100.5 cm^{-1}), which is much higher than the graphite value (15-23 cm^{-1}), indicating that the crystallinity of the ACO sample is much lower than the graphite [23]. The value of the average lateral sizes (L_a), calculated from Raman data by using Equation 1 [23], is 2.42 nm.

$$L_a = C(\lambda_L)\frac{I_G}{I_D} \tag{1}$$

In equation 1, I_D and I_G are areas of D band and G band, respectively, and $C(\lambda_L)=C_o+\lambda_L C_1$. Where, C_o is equal to -12.6 nm; λ_L is the wavelength and C_1 is equal to 0.033.

Fig. 2 shows the X ray diffraction profile (XRD) of the ACO sample, where one can see broad peaks centered at 24.86 and 44.05 ° (2θ), which are associated to Muller index of (002) and (101) [24]. These peaks are characteristics of a turbostratic structure of graphite micro crystallites and they mean that ACO has an intermediate structure between amorphous carbon and graphite [23].

Using Gaussian deconvolution on XRD data, one could use the peak at 24.86 °to estimate both the spacing of aromatic ring layers (d_{002}) and the crystallite thickness (L_c) [25]. However, the average lateral size (L_{a-XRD}) of the crystallites was determined using the peak at (101) [25]. The d_{002} (0.352 nm) was calculated using Bragg's law and the crystallite size L_c (0.601 nm) and L_{a-XRD} (2.60 nm) were determined using Scherrer's equation [25]. The value of d_{002} (0.352 nm) was higher than the one of pure graphite (0.336-0.337 nm), due to a lower crystalline degree of the ACO sample in relation to the graphite [23]. It can be observed several sharp and less intense peaks besides peaks at 24.86 and 44.05 ° (2θ), which may be related to inorganic materials that were already present in the biomass. Comparing the value of L_a previously determined by

Raman spectroscopy (2.42) with that determined by XRD (2.60), it can be concluded that they are very close. Nevertheless, the L_a determination by XRD is considered much more accurate than the Raman spectroscopy one [23].

The morphology of the ACO sample can be observed in Fig. 3A and 3B.

(A)   (B)
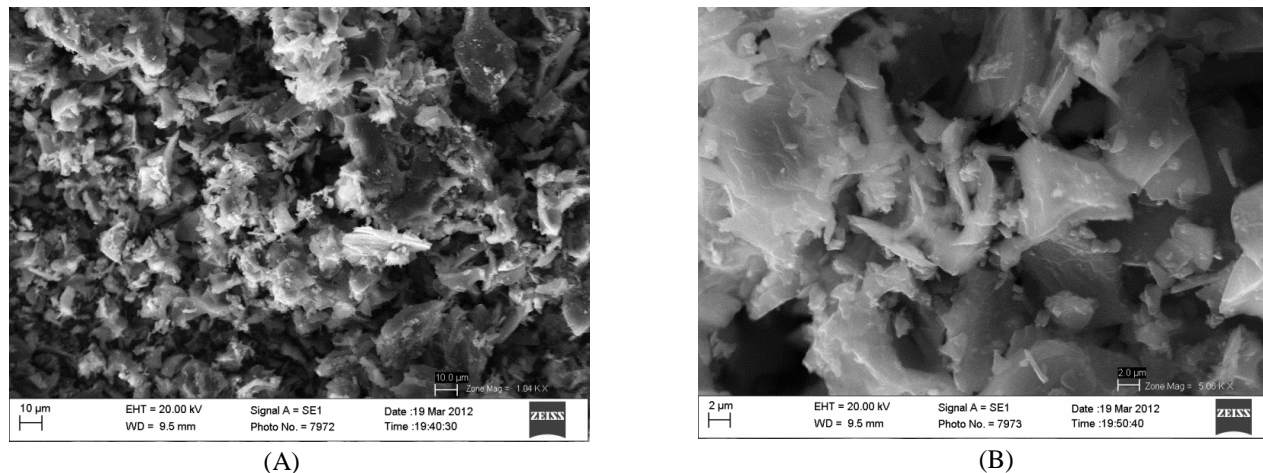
FIGURE 3. SEM IMAGES OF THE ACO AT DIFFERENT ENLARGEMENTS

These Figures show that the particles are non-uniform, i.e. without a predominant form. In addition, Fig. 3B shows that the ACO has a lamellar structure.

Energy dispersive spectroscopy (EDS) was used to determine the chemical composition of the ACO sample and its results are shown in Table 2.

TABLE 2
RESULTS OF ENERGY DISPERSIVE SPECTROSCOPY (EDS) MEASUREMENTS

	Element								
	C	O	Mg	P	S	Cl	K	Ca	Fe
% Weight	65.0	18.0	0.4	1.2	0.5	0.2	7.8	6.6	0.3
% Atomic	77.5	16.0	0.3	0.5	0.2	0.1	2.9	2.4	0.1

This table shows that the ACO is constituted of several elements, such as: magnesium, phosphorus, surfer, chlorine, potassium, calcium, and iron. According to [26] and [27], most of these elements are a characteristic of the orange peel composition. The concentration of potassium (2.9 %) and calcium (2.4 %) is much higher than the others, but their concentrations are considered normal in Brazilian oranges. The presence of oxygen is an indication that the ACO had a lot of oxygenated groups on its surface.

3.2   Adsorption

The kinetic data of phenol adsorption onto the ACO are shown in Fig. 4.
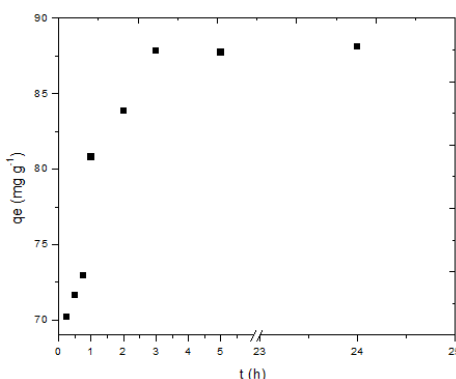
FIGURE 4. CONTACT TIME EFFECT ON ADSORBED PHENOL CONCENTRATION

For the ACO, the contact time of 3 hs is needed to establish the phenol adsorption equilibrium. At this stage, the adsorbed phenol amount is 88 mg g^{-1}, i.e. 19 % of the initial amount. The kinetic data were fitted using pseudo first-order and pseudo second-order kinetic models [28]. The kinetic results are shown in Table 3. It can be observed from Table 3 that the correlation coefficient (R^2) for pseudo first-order kinetic model (0.88) was much lower than R^2 for the pseudo-second order model (1.00), indicating that the kinetic of adsorption process is more accurately represented by the pseudo second-order kinetic model. In addition, the comparison between the equilibrium concentration obtained from Fig. 4 (qe = 88 mg g^{-1}) and that one from pseudo-first order (qe = 23.60 mg g^{-1}) and from pseudo-second order (qe = 87.64 mg g^{-1}) reinforces that the adsorption kinetic process of phenol onto the ACO can be described by a pseudo-second order model.

TABLE 3
KINETIC PARAMETERS OF PHENOL ADSORPTION ON THE ACO

C_0 (mg L^{-1})	Pseudo first-order			Pseudo second-order		
	K_1 (h^{-1})	q_e (mg g^{-1})	R^2	K_2 (h^{-1})	q_e (mg g^{-1})	R^2
1000	0.92	23.60	0.88	0.11	87.64	1.00

Fig. 5 shows the adsorption percentage (%) and adsorption capacity (q$_e$) of the phenol as a function of the ACO dosage, where the ACO dosage ranged from 0.01 to 0.5 g.
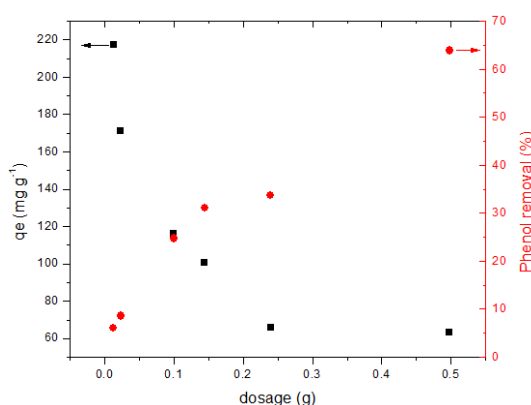
FIGURE 5. EFFECT OF ADSORBENT DOSE ON THE ADSORPTION OF PHENOL ONTO THE ACO

It can be observed that the phenol removal (%) and the phenol adsorption capacity (qe) depend strongly on the ACO dosage. However, these two properties have distinct dependence on the ACO dosage, i.e. the removal efficiency increased with the dosage while the adsorption capacity decreased. The former may happen due to an increase in the adsorption sites with an increase in the ACO dosage [29]. Nevertheless, a higher adsorbent dose results in a lower adsorption capacity due to overcrowding of adsorbent particles, resulting in a decrease in the availability of adsorption sites [7]. In order to carry out further studies we have to choose a "work dosage", in which both the equilibrium concentration and the removal amount have meaningful values. Consequently, in the next studies, an ACO dosage of 0.1 mg g^{-1} will be used.

The effect of pH on phenol adsorption is showed in Fig. 6.
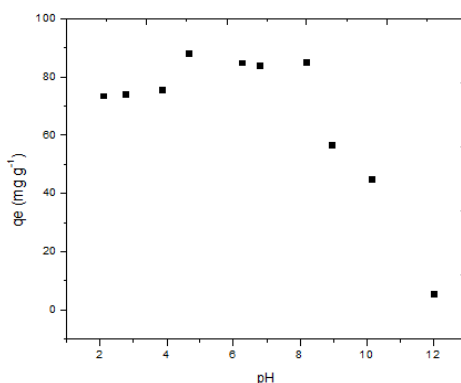
FIGURE 6. EFFECT OF SOLUTION pH ON THE ADSORPTION OF PHENOL ONTO THE ACO

It can be observed that the value of qe is almost the same in the pH range from 2 to 4. After that, i.e. pH > 4, the phenol adsorption increases with an increase in pH up to 4.5, then the phenol adsorption remains constant until pH ~ 8 and thereafter the phenol adsorption decreases. The increase in the phenol adsorption after pH 4 results from the decrease in hydrogen ion concentration in solution [8]. These ions are adsorbed in basic sites, resulting in a decrease in the basic site interactions of the ACO surface with phenol molecules [8]. In other words, the decrease in hydrogen ion concentration in a solution with a pH increase, results in an increase in the site number available for phenol adsorption. The phenol adsorption reaches its maximum value at a pH range from 4.5 to 8 because phenol is undissociated and the dispersion interaction is predominant [14].The decrease in qe value between pH 8 and 10 is given by an increase in OH$^-$ ions quantity [30]. The OH$^-$ ions in the solution are adsorbed on the positively charged ACO surface (pH$_{pzc}$ = 10.5), which reduces the undissociated phenol-ACO surface interaction. At pH >10.5 the phenol adsorption decreases abruptly, probably, due to electrostatic repulsion between the negatively charged ACO surface and the anionic form of the phenol molecules (pK$_a$ = 9.9) in the solution [30,31].

Fig. 7 and Table 4 shows the results of fitted experimental data to Langmuir and Langmuir-Freundlich (Sips) equations [32].
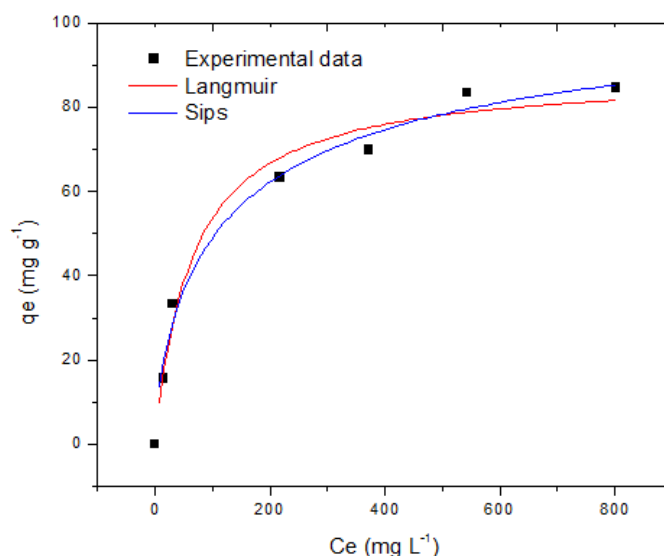
FIGURE 7. ADSORPTION ISOTHERM OF PHENOL ONTO THE ACO

It can be seen that the R^2 related to Langmuir and Langmuir-Freundlich model is quite high and the same. Considering that the adsorption process follows the Langmuir model (the simplest one), the maximum phenol adsorption capacity of ACO is 88 mg g^{-1} and the adsorption occurs in a monolayer [33].

TABLE 4
ADSORPTION ISOTHERM CONSTANTS FOR PHENOL ONTO THE ACO

Langmuir isotherm			Langmuir-Freundlich (Sips) isotherm			
b (L mg^{-1})	Q$_m$ (mg g^{-1})	R^2	b (L mg^{-1})	Q$_m$ (mg g^{-1})	α	R^2
0,02	88	0.97	0.03	111	0.69	0.97

Thus, orange peels must be considered an excellent source of biomass to produce the phenol adsorbent, taking into account their great availability, their environmental disposal problems and their considerable phenol adsorption capacity.

IV.   CONCLUSION

The ACO has a turbostratic structure and is mainly constituted by micropores. The sample presents inorganic impurities in its composition and has a basic character in water. The optimum dosage was 0.1 g/50 cm^3 of phenol solution and the optimum pH range was between 4 and 8. The phenol adsorption onto the ACO followed a pseudo second order model and its monolayer adsorption capacity was 88 mg g^{-1}.

REFERENCES

[1]   J.J.T. Gama, C.M. Sylos, Major carotenoid composition of Brazilian Valencia orange juice: Identification and quantification by HPLC, Food Res. Int. 38 (2005) 899–903.

[2]   H.R.M. Barros, T.A.P.C. Ferreira, M.I. Genovese, Antioxidant capacity and mineral content of pulp and peel from commercial cultivars of citrus from Brazil, Food Chem. 134 (2012) 1892–1898.

[3]   M.T.P.S. Clerici, Nutritional bioactive compounds and technological aspects of minor fruits grown in Brazil, Food Res. Int. 44 (2011) 1658–1670.

[4]   L.D. Fiorentin, B.T. Menon, S.T.D. Barros, N.C. Pereira, O.C.M. Lima, A.N. Modenes, Isotermas de sorção do resíduo agroindustrial bagaço de laranja, Rev. Bras. Eng. Agrícola E Ambient. 14 (2010) 653–659.

[5]   A.M. Alexandrino, H.G. De Faria, C. Giatti, M. De Souza, R.M. Peralta, Aproveitamento do resíduo de laranja para a produção de enzimas lignocelulolíticas por Pleurotus ostreatus (Jack : Fr), Ciência E Tecnol. Aliment. 27 (2007) 364–368.

[6]   M.E.R. Cantu, Journal of Analytical and Applied Pyrolysis Pyrolysis of sweet orange (Citrus sinensis) dry peel, 86 (2009) 245–251.

[7]   L.A. Rodrigues, M.L.C.P. da Silva, M.O. Alvarez-Mendes, A.R. Coutinho, G.P. Thim, Phenol removal from aqueous solution by activated carbon produced from avocado kernel seeds, Chem. Eng. J. 174 (2011) 49–57.

[8]   Q.-S. Liu, T. Zheng, P. Wang, J.-P. Jiang, N. Li, Adsorption isotherm, kinetic and mechanism studies of some substituted phenols on activated carbon fibers, Chem. Eng. J. 157 (2010) 348–356.

[9]   L.A. Rodrigues, T.M.B. Campos, M.O. Alvarez-Mendes, A.R. Coutinho, K.K. Sakane, G.P. Thim, Phenol removal from aqueous solution by carbon xerogel, J. Sol-Gel Sci. Technol. (2012).

[10] K. Lin, J. Pan, Y. Chen, R. Cheng, X. Xu, Study the adsorption of phenol from aqueous solution on hydroxyapatite nanopowders., J. Hazard. Mater. 161 (2009) 231–40.

[11] X. Zeng, Y. Fan, G. Wu, C. Wang, R. Shi, Enhanced adsorption of phenol from water by a novel polar post-crosslinked polymeric adsorbent., J. Hazard. Mater. 169 (2009) 1022–8.

[12] L.A. Rodrigues, L.A. Sousa Ribeiro, G.P. Thim, R.R. Ferreira, M.O. Alvarez-Mendez, A.D.R. Coutinho, Activated carbon derived from macadamia nut shells: an effective adsorbent for phenol removal, J. Porous Mater. (2012).

[13] G. Dursun, H. Ciçek, A.Y. Dursun, Adsorption of phenol from aqueous solution by using carbonised beet pulp., J. Hazard. Mater. 125 (2005) 175–82.

[14] B.H. Hameed, a a Rahman, Removal of phenol from aqueous solutions by adsorption onto activated carbon prepared from biomass material., J. Hazard. Mater. 160 (2008) 576–81.

[15] A. Bhatnagar, M. Sillanpää, Utilization of agro-industrial and municipal waste materials as potential adsorbents for water treatment—A review, Chem. Eng. J. 157 (2010) 277–296.

[16] J.C. Moreno-Piraján, L. Giraldo, Heavy Metal Ions Adsorption from Wastewater Using Activated Carbon from Orange Peel, E-Journal Chem. 9 (2012) 926–937.

[17] L. Wang, J. Zhang, A. Wang, Removal of methylene blue from aqueous solution using chitosan-g-poly(acrylic acid)/montmorillonite superadsorbent nanocomposite, Colloids Surfaces A Physicochem. Eng. Asp. 322 (2008) 47–53.

[18] L.A. Rodrigues, L.J. Maschio, R.E. da Silva, M.L.C.P. da Silva, Adsorption of Cr(VI) from aqueous solution by hydrous zirconium oxide., J. Hazard. Mater. 173 (2010) 630–6.

[19] H. Boehm, Some aspects of the surface chemistry of carbon blacks and other carbons, Carbon N. Y. 32 (1994) 759–769.

[20] L. Zhu, Y. Deng, J. Zhang, J. Chen, Adsorption of phenol from water by N-butylimidazolium functionalized strongly basic anion exchange resin., J. Colloid Interface Sci. 364 (2011) 462–8.

[21] K.S.W. Sing, D.H. Everett, R.A.W. Haul, L. Moscou, R.A. Pierotti, J. Rouquérol, T. Siemieniewska, Reporting physisorption data for gas/solid systems with special reference to the determination of surface area and porosity (Recommendations 1984), Pure Appl. Chem. 57 (1985) 603–619.

[22] C.M.L. Barbosa, M.T.C. Sansiviero, Decomposição térmica de complexos de Zn e Cd com isomaleonitriladitiolato (imnt), Quim. Nova. 28 (2005) 761–765.

[23] O.O. Sonibare, T. Haeger, S.F. Foley, Structural characterization of Nigerian coals by X-ray diffraction, Raman and FTIR spectroscopy, Energy. 35 (2010) 5347–5353.

[24] S.-S. Tzeng, K.-H. Hung, T.-H. Ko, Growth of carbon nanofibers on activated carbon fiber fabrics, Carbon N. Y. 44 (2006) 859–865.

[25] D. Li, H. Wang, X. Wang, Effect of microstructure on the modulus of PAN-based carbon fibers during high temperature treatment and hot stretching graphitization, J. Mater. Sci. 42 (2007) 4642–4649.

[26] A. K. Bejar, N. B. Mihoubi, N. Kechaou, Moisture sorption isotherms – Experimental and mathematical investigations of orange (Citrus sinensis) peel and leaves, Food Chem. 132 (2012) 1728–1735.

[27] A.U. Mahmood, J. Greenman, A.H. Scragg, Orange and potato peel extracts: Analysis and use as Bacillus substrates for the production of extracellular enzymes in continuous culture, Enzyme Microb. Technol. 22 (1998) 130–137.

[28] L.A. Rodrigues, M.L.C.P. da Silva, Thermodynamic and kinetic investigations of phosphate adsorption onto hydrous niobium oxide prepared by homogeneous solution method, Desalination. 263 (2010) 29–35.

[29] A. Shukla, Y.-H. Zhang, P. Dubey, J.L. Margrave, S.S. Shukla, The role of sawdust in the removal of unwanted materials from water., J. Hazard. Mater. 95 (2002) 137–52.

[30] H.B. Senturk, D. Ozdes, A. Gundogdu, C. Duran, M. Soylak, Removal of phenol from aqueous solutions by adsorption onto organomodified Tirebolu bentonite: equilibrium, kinetic and thermodynamic study., J. Hazard. Mater. 172 (2009) 353–62.

[31] M.H. El-Naas, S. a Al-Muhtaseb, S. Makhlouf, Biodegradation of phenol by Pseudomonas putida immobilized in polyvinyl alcohol (PVA) gel., J. Hazard. Mater. 164 (2009) 720–5.

[32] V.V.S. Guilarduci, J.P. Mesquita, P.B. Martelli, H.F. Gorgulho, Adsorção de fenol sobre carvão ativado em meio alcalino, Quim. Nova. 29 (2006) 1226–1232.

[33] L.A. Rodrigues, M.L.C.P. Silva, Adsorption kinetic, thermodynamic and desorption studies of phosphate onto hydrous niobium oxide prepared by reverse microemulsion method, Adsorption. 16 (2010) 173–181.